

## Floods in a changing climate: Does the past represent the future?

Shaleen Jain

Cooperative Institute for Research in Environmental Sciences and NOAA-CIRES Climate Diagnostics Center  
University of Colorado, Boulder, Colorado, USA

Upmanu Lall

Department of Earth and Environmental Engineering and International Research Institute for Climate Prediction  
Columbia University, New York, New York, USA

**Abstract.** Hydrologists have traditionally assumed that the annual maximum flood process at a location is independent and identically distributed. While nonstationarities in the flood process due to land use changes have long been recognized, it is only recently becoming clear that structured interannual, interdecadal, and longer time variations in planetary climate impart the temporal structure to the flood frequency process at flood control system design and operation timescales. The influence of anthropogenic climate change on the nature of floods is also an issue of societal concern. Here we focus on (1) a diagnosis of variations in the frequency of floods that are synchronous with low-frequency climate state and (2) an exploration of limiting flood probability distributions implied by a long simulation of a model of the El Niño/Southern Oscillation. Implications for flood risk analysis are discussed.

### 1. Introduction

The assumption that annual maximum floods are independent and identically distributed is central to most flood frequency and risk analyses. While the role of urbanization in changing flood frequency has long been recognized, it is only recently that the influence of the slowly changing climate on flood frequency has attracted interest [e.g., *Booy and Morgan, 1985; Robson et al., 1998; National Research Council, 1998, 1999; Olsen et al., 1999; Jain and Lall, 2000; Walker and Stedinger, 2000*]. In this paper, we consider the potential impact of quasiperiodic interannual and interdecadal variations in climate (e.g., the El Niño/Southern Oscillation) on flood frequency. Anthropogenic factors are not considered.

The El Niño/Southern Oscillation (ENSO) represents the dominant coupled ocean-atmosphere mode of the tropical Pacific [*Cane, 1992*]. The oceanic component of this phenomenon, El Niño, and its atmospheric counterpart, Southern Oscillation, exhibit covariability at 2 to 7-year timescales. However, there have been substantial variations in ENSO frequency, intensity, and duration over the last century. On interannual timescales a significant fraction of the global climatic variability can be associated with ENSO. In the Northern Hemisphere winter, up to 30% of the observed variance of the large-scale atmosphere circulation can be attributed to ENSO [*Horel and Wallace, 1981; Trenberth et al., 1998*]. The global impacts of ENSO primarily stem from the changes in the strength and location of tropical Pacific convection that, in turn, trigger changes in the global atmospheric circulation [*Cane and Clement, 1999*]. The ENSO extreme phases are often associated with major episodes of floods and droughts [e.g., *Trenberth and Guillemot, 1996; Barlow et al., 2001*] in many locations worldwide. The Pacific Decadal Oscillation (PDO), identified as the leading eigenvector of North Pacific

sea surface temperature variability [*Mantua et al., 1997*], shows marked low-frequency structure, with “regime-like” variations at interdecadal timescales. ENSO and PDO are known to modulate the temperature, precipitation, and streamflow patterns across the United States [e.g., *Cayan et al., 1999; Ropelewski and Halpert, 1987; Dracup and Kahya, 1994; Mantua et al., 1997; Gershunov and Barnett, 1998; Dettinger et al., 2000; Rajagopalan et al., 2000*]. The strength of these teleconnections varies spatially and also over periods of decades [*McCabe and Dettinger, 1999; Cole and Cook, 1998; Mann et al., 2000*]. The inherent quasi-oscillatory nature of ENSO and PDO seen in the instrumental record has been further substantiated by the recent work based on long proxy climate records [*D’Arrigo et al., 1999; Urban et al., 2000*]. This reinforces the view that present and future hydroclimatic variations may be synchronous with these key global climate indicators. However, there is some debate as to whether ENSO and PDO are distinct climate modes or are different space-time components of the same low-frequency phenomena [*Zhang et al., 1996, 1997; Barlow et al., 2001*].

Interannual-to-interdecadal climate modes (ENSO and PDO) may affect floods by markedly changing patterns of atmospheric moisture transport in the flood season hence changing the probabilities of floods in a given year at a particular location. Such changes may be reflected in corresponding variations in the total snowpack and the storm rainfall and duration, as well as antecedent soil moisture conditions. Some of these connections were explored by *Jain and Lall [2000]*. If such changes are quasiperiodic, then a flood record of sufficient length (greater than the period of the oscillation) may still accurately reflect long-term flood exceedance probabilities that are used for flood control design. On the other hand, a better understanding of the nature of the quasiperiodic variations in flood frequency or the clustering of major floods across years may be of value for the operation of large multipurpose reservoir systems. To this end some specific questions are as follows.

Copyright 2001 by the American Geophysical Union.

Paper number 2001WR000495.  
0043-1397/01/2001WR000495\$09.00

1. How can changes in flood frequency be quantified and related to oscillatory modes (e.g., ENSO and PDO) of climate?
2. Is there evidence of interannual clustering in floods that is related to an underlying slowly varying climate state?
3. Can an observational record of limited length be taken to be representative of future flood sequences? What length of record may be needed to accept the paradigm that the distribution of floods is stationary?
4. What can we say about the long-term variations (greater than the typical 3- to 7-year band quasiperiodic behavior) in ENSO and their implications for floods? Can the previous 30 ( $N$ ) years be considered representative of the next 30 ( $N$ )?

The seasonal hydrology of the Pacific Northwest region is apparently well connected to both the PDO and the ENSO [Cayan, 1996; Mantua *et al.*, 1997]. We explore a data set from the Pacific Northwest where the annual flood mechanism is linked to large-scale atmospheric moisture flow rather than dominated by local convection. We choose a relatively long record (88-year-long flood record for the Similkameen River in Washington), rather than a regional analysis, to illustrate ways in which the temporal variations in flood frequency (and resulting nonstationarity) can be diagnosed. This site is particularly suited for a diagnostic study of the interannual-to-interdecadal climate influences on flood magnitudes because of its location in an ENSO- and PDO-sensitive region and a long record with minimal flow regulation. Annual maximum floods occur between late April and June and are predominantly due to snowmelt or rain on snow. Frontal winter/spring precipitation is thus the source of floods providing a homogeneous record as far as the flood-generating mechanism. We also consider a hypothetical situation for insights on limiting distributions of floods under quasiperiodic climate variations, where a flood series is presumed to closely follow the strength of ENSO (as measured by the NINO3 index) constructed from an 110,000-year run with stationary forcing of the Zebiak and Cane [1987] coupled ocean-atmosphere ENSO model.

## 2. Data and Site Information

The 1911–1998 record for annual maximum floods on Similkameen River near Nighthawk, Washington (U.S. Geological Survey (USGS) station number 12442500), is listed as minimally affected by diversions and human influences [Slack *et al.*, 1992]. The drainage area of this gauge is 9192 km<sup>2</sup> (3550 miles<sup>2</sup>). The USGS gauging station is located at 347 m (1138 feet) above the National Geodetic Vertical Datum. Similkameen River (gauge location of 48°59′05″N, 119°37′02″W) is part of the upper Columbia River basin. The median flood for the period of record is 456 m<sup>3</sup>/s (16,100 cfs) and the maximum and minimum recorded floods are 1296 m<sup>3</sup>/s (45,800 cfs) and 134 m<sup>3</sup>/s (4750 cfs), respectively. The median date of the annual maximum flood is May 28, with late April to late June as the range of dates for the 88 years of record analyzed. The highest (lowest) floods on record occurred in years with negative (positive) NINO3 and PDO indices. The flood data were log transformed prior to all the analyses reported in this paper.

The NINO3 and PDO data sets were acquired from the National Oceanic and Atmospheric Administration Climate Prediction Center (<ftp://ftp.ncep.noaa.gov/pub/cpc/wd52dg/data/indices/sstoi.indices>) and the University of Washington (<http://www.atmos.washington.edu/~mantua/abst.PDO.html>), respectively. The NINO3 index is computed as an average of sea surface temperature over the eastern tropical Pacific (~5°S–5°N, 90°W–

150°W). It is based on blended ship, buoy, and bias-corrected satellite data. The PDO index is the leading eigenvector of North Pacific sea surface temperatures. The interdecadal mode has been emphasized by the presence of regime-like periods over the instrumental record (1870–1889, 1890–1924, 1925–1947, 1948–1976, and 1977–1990). For the analysis presented here, we have used the average winter season (December–February) NINO3 and PDO anomalies.

A NINO3 index derived from an 110,000-year integration of a coupled ocean-atmosphere model for ENSO [see Zebiak and Cane, 1987; Cane, 1992; Clement and Cane, 1999] was also used. The model run had stationary climate forcings, and model results may be considered representative of the natural variability of the coupled ocean-atmosphere system for the tropical Pacific. The mean annual NINO3 index for the coupled model run is 0.38 K. Annual average NINO3 index values are used for the analysis in this paper.

## 3. Analysis

In this section we first analyze the historical flood record for the Similkameen River and explore possible associations with the large-scale climate indices. Next, we conduct a moving window analysis of the flood record to examine the nonstationary behavior and persistence of floods (across select quantiles) in time. Since ENSO exhibits variations at multiple timescales, a wavelet analysis is carried out to assess the nonstationary structure of ENSO and its implications for the flood frequency distribution. Finally, we assess the long-term variations in ENSO using results from a coupled ocean-atmosphere model of ENSO [Zebiak and Cane, 1987].

## 4. Similkameen River Floods: Variability and Climate Connections

A 30-year period is often considered to represent the climate of a region [Guttman, 1989]. It is also longer than the interannual and interdecadal oscillatory variations of interest here. We will consider it to be the shortest window over which to assess the stationarity or variability of the flood and climate records. The historical record of Similkameen River annual maximum floods along with 30-year moving window means (estimated using robust local linear regression [Loader, 1999]) of the flood series is shown in Figure 1a. There is considerable year-to-year variability about the interdecadal variations seen through the smoothed estimate. The 1950–1975 period recorded some of the highest floods for the Similkameen River. The smoothed variations of the NINO3 and PDO over the last century are shown in Figure 1b. Interestingly, the 1950–1975 period was marked by persistent negative anomalies for both the NINO3 and PDO. These coincidental trends between the Similkameen River high floods and the climate indices suggest a possible influence of the large-scale climate on the flood potential for the Similkameen River.

A correlation analysis suggests a statistically significant relationship between Similkameen River annual maximum floods and both winter (December–February) NINO3 and the PDO indices. The null hypothesis that these correlations are zero is rejected based on a two-sided  $t$  test, since the probabilities in favor of the hypothesis are  $10^{-4}$  and  $2 \times 10^{-5}$ , respectively. These statistics are summarized in Table 1. The reader may note from Table 1 that the partial correlations [Conover, 1999, pp. 327–328] of flood flows with NINO3 and

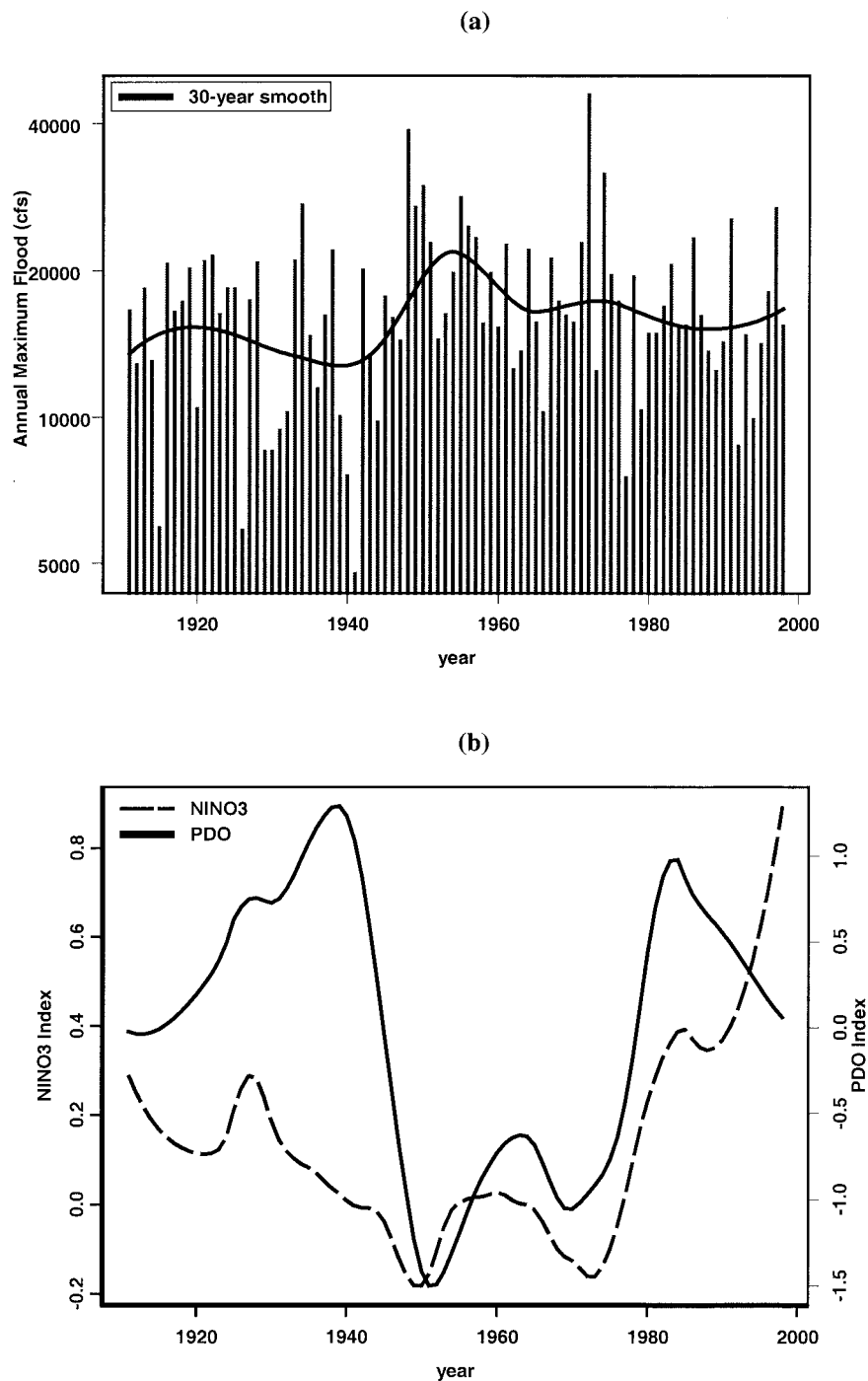


**Figure 1.** (a) Historical record (1911–1998) for the annual maximum floods on Similkameen River. (b) Long-term variations in the key climate indices for the winter season (December–February): NINO3 (dashed line) and Pacific Decadal Oscillation (PDO) (solid line). The 30-year smoothed estimates are based on robust local regression [Hastie and Loader, 1993; Loader, 1999].

PDO, given the other variable, are also statistically significant, suggesting that both the tropical and extratropical factors and the different timescales of climatic evolution represented by these indices are apparently important. The linkage of the climate indices to floods becomes clearer upon examining the NINO3 and PDO anomalies corresponding to the 10 smallest and largest Similkameen River floods over the historical record (see Table 2). Low (high) floods are highly favored in years with positive (negative) NINO3 and PDO anomalies for the

December–February period. These results are consistent with the observation of *Cayan et al.* [1999] that winters are dry and warm in the Pacific Northwest during El Niño years. Another noteworthy aspect is that the climate indices used are averaged over the December–February period, while the typical date of flood occurrence is late May. Consequently, these correlations suggest prospects for the seasonal prediction of flood risk.

Flood control managers are more interested in the behavior of extreme floods than in the mean annual flood and its vari-

**Table 1.** Correlation Between Similkameen River Annual Maximum Floods (Log Transformed) and the Winter (December–February) Climate Indices<sup>a</sup>

Climate Index	Correlation With Floods
NINO3	-0.39 (0.0001)
NINO3/PDO	-0.27 (0.015)
PDO	-0.44 (0.0001)
PDO/NINO3	-0.33 (0.001)

<sup>a</sup>The floods typically occur in late May. On the basis of a two sided  $t$  test all correlations are significantly different from zero at the  $p = 0.05$  level. Partial correlations computed as  $r_{xy|z} = (r_{xy} - r_{xz}r_{yz})/\sqrt{(1 - r_{xz}^2)(1 - r_{yz}^2)}$  are shown for NINO3 (removing the effects for PDO dependence) and PDO (removing the effects for NINO3 dependence). The numbers in parentheses represent the  $p$  value for the null hypothesis that a correlation is 0, based on a  $t$  test with  $(n - 2)$  degrees of freedom for the correlation and  $(n - 3)$  degrees of freedom for a partial correlation.

ations, so it is interesting to explore how the annual extremes (flood quantiles) have varied at this site over the last century. We approach this nonparametrically by considering the threshold exceedance process (as a nonhomogeneous Poisson process) and then estimating the time-varying rate of threshold exceedance using a 40-year moving window. The thresholds considered are four percentiles (90th, 67th, 33rd, and 10th) of the data computed from the full 88-year record. On average, these percentiles will be exceeded 10, 33, 67, and 90% of the time. The time-varying (moving window) probability of exceedance of each threshold is estimated using a weighted local regression of a binary (0, 1) annual threshold exceedance indicator versus calendar year. The results are presented in Figure 2. The 1940–1970 period stands out as one in which the frequency of exceedance of the entire flood distribution moves toward higher exceedance probabilities. Interestingly, this is a period when both the NINO3 and the PDO indices record a persistent negative anomaly from their mean state (Figure 1b). At this level of filtering the two climate indices evolve quite coherently in time, suggesting that larger-scale low-frequency dynamic variations in the climate system may be modulating their state. Also, Mantua *et al.* [1997] note that there appears to be a spatiotemporal coherence between ENSO and PDO (however, the causal link is not clear). Consequently, the large-scale Northern Hemisphere atmospheric circulation patterns show associations with both the interannual (ENSO) and in-

**Table 2.** Statistics of PDO and NINO3 (December–February) Anomalies Corresponding to the 10 Smallest and Largest Floods Over the Similkameen River Historical Record<sup>a</sup>

	Ten Smallest Floods	Ten Largest Floods
Median NINO3 anomaly	1.05	-0.42
Interquartile range NINO3 anomaly	1.09	0.56
Median PDO anomaly	1.18	-1.84
Interquartile range PDO anomaly	1.13	2.01

<sup>a</sup>Here we report the median (50th percentile) and interquartile range (difference between the 25th and the 75th percentile) of the climate indices. A “two-sided”  $t$  test indicated that the null hypothesis that the population means are the same during high and low flood years was rejected for both NINO3 ( $p = 0.0003$ ) and PDO ( $p = 0.0002$ ).

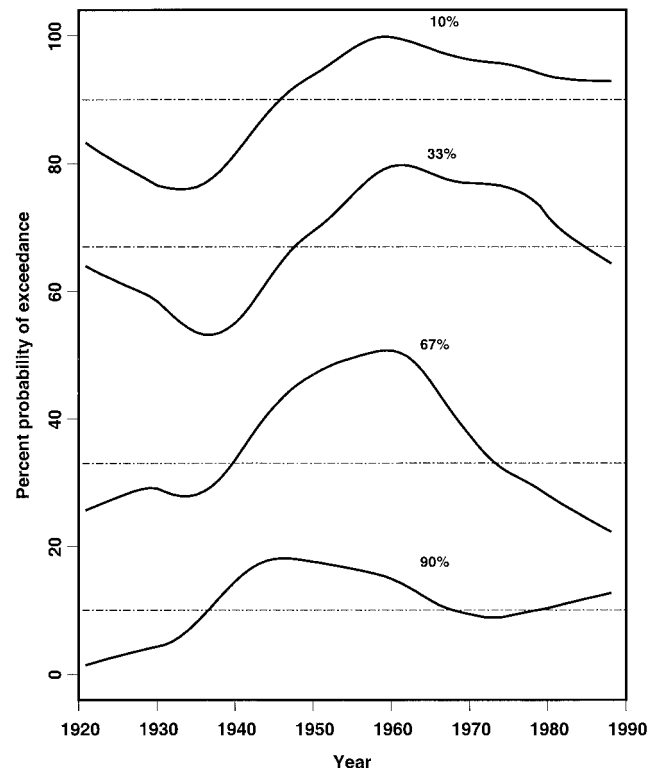


**Figure 2.** Trends in some key percentiles (10th, 33rd, 67th, and 90th) of the annual maximum flood for the Similkameen River. The trends were estimated nonparametrically using local regression of a threshold exceedance process with a 40-year window. The estimates near the ends of the flood record may be discounted since they have higher variance. Dashed-dotted lines represent the percentiles estimated from the full record that correspond to the threshold exceeded. Changes in the “spread” and monotonic trends in these percentiles reflect changes in the underlying probability distribution as a response multidecadal-to-secular forcings, which, in turn, may modulate the interannual (e.g., El Niño) modes.

terdecadal (PDO) modes of climate and influence the precipitation and temperature patterns over the continents. In the context of the climate-flood connections, persistent ENSO and PDO anomalies (as seen during the past century (Figure 1)) have the potential to (1) impart regime-like structure to the flood record and (2) favor persistent flood anomalies (seen as spells of high/low floods lasting over a long period). For the Similkameen River the differences in the right (higher-percentile thresholds) and left tail (lower-percentile thresholds) of the flood distribution over different epochs (pre-1940 and post-1970) are also evident. The trends in the two tails are of opposite sign in the pre-1940 period suggesting an increased variance in the interannual flood process during that period. Higher floods in the post-1940 period are consistent with the 1948–1976 PDO regimes identified from records. The 1940 switch in the flood and smoothed PDO and NINO3 trends has also been noted for a number of other climate records [Ghil and Vautard, 1991; Minobe, 1997; Jain *et al.*, 1999]. Further, a broad region across the United States (including the Pacific Northwest) also shows spring temperature shifts consistent with a larger-scale 50- to 70-year climatic variation [Minobe, 1997].

## NINO3

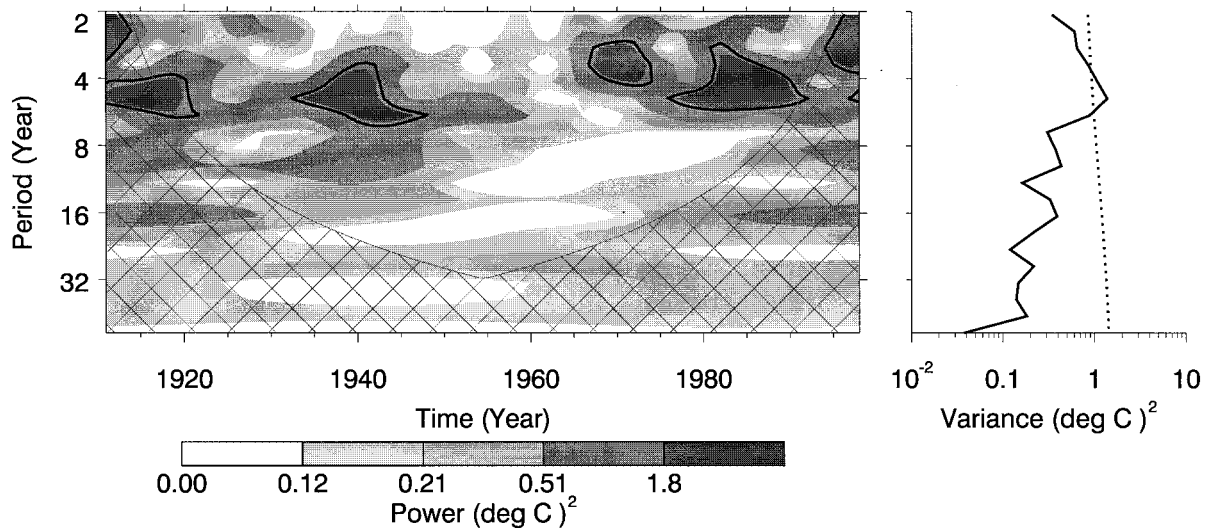


**Figure 3.** Wavelet power spectrum for NINO3. The contour levels are chosen so that 75%, 50%, 25%, and 5% of the wavelet power is above each level, respectively. The cross-hatched region shows the cone of influence, where zero padding has reduced the variance. Solid contours mark significant spectral power at the 10% level (with global wavelet spectrum as the background). On the right is the global wavelet power spectrum (solid line). The dotted line is the 10% significance level for the global wavelet spectrum relative to a red-noise background. Wavelet analysis is based on *Torrence and Compo* [1998].

### 5. Long-Term Variations in the Estimated Flood Frequency Distribution

In the context of understanding the long-term variations in flood frequency it is useful to understand the long-term mean and distribution changes in key climate precursors (such as, ENSO). ENSO is a quasiperiodic phenomenon originating in the tropical Pacific, with marked periodicity on 2- to 7-year timescales. Here, using wavelet analysis, we focus on the nature of instrumental and model ENSO variations and their time and frequency variations. Wavelet analysis [*Kaiser, 1994; Torrence and Compo, 1998*] provides a means to decompose the changing nature of oscillatory patterns as a function of time. Thus we can diagnose how the higher-frequency structure of ENSO about the 30-year moving window mean shown in Figure 1b is manifest as a function of time, without a priori specification of the span of different moving windows to identify these variations. We first examine (Figure 3) how the time-frequency structure of ENSO may have evolved over the historical period. We note that the dominant frequency associated with NINO3 has undergone changes over the period of record, that is, 4–8 years during the pre-1920 period, 3–15 years during the 1920s–1940s, weak interannual activity during 1950–1970, and 2–8 years with an increase in the frequency band to include longer-term variations in the post-1970 period. This time variation of dominant ENSO frequencies has often manifested as episodes of anomalous ENSO activity, like the protracted 1991–1995 El Niño event, the 1997 “El Niño of the century,” and the relatively inactive 1940–1970 period (climatological variations and modest La Niña events). As seen through analysis presented in sections 3 and 4, the dependence of floods on ENSO suggests that the long-term variations in select climate precursors (we consider ENSO for our analysis)

will likely be mirrored as flood frequency fluctuations (often as structured nonstationarities). Thus our exploratory understanding of the climate-flood relationships leads us to the following questions: (1) Is the historical record a representative of the possible time-frequency fluctuations of the climate system? (2) How informative are the limited-length flood records of future changes in flood frequency?

As has been noted in recent studies, there is some question whether the decadal-scale changes in the tropical Pacific (changes in the ENSO frequency and amplitude) (1) are related to the North Pacific (associated with PDO) variations [e.g., *Gu and Philander, 1997*], (2) reflect changes in the structure of the climate system [*Trenberth and Hoar, 1996; Rajagopalan et al., 1997*], or (3) are natural modes of the climate system. While these are open questions, it is useful to see what may be indicated for long-term variations of hydroclimatic extremes by a nonlinear, tropical ocean-atmosphere model that specifically models ENSO dynamics. We used a 110,000-year integration of the *Zebiak and Cane* [1987] (ZC) model of ENSO under stationary climate forcing (no CO<sub>2</sub> changes, no orbital effects, etc.) to explore the potential nature of long-term variability of climate and how it may translate into nonstationarity or long memory in the flood process. The ZC model [*Zebiak and Cane, 1987; Cane and Clement, 1999*] provided the first long-range forecast of an El Niño event and is generally considered as having plausible physics for the multi-scale feedback of the ocean and the atmosphere in the tropical Pacific. The atmospheric and ocean components of the ZC model are based on linear shallow water equations, and the Kelvin and Rossby wave dynamics of the tropical Pacific relevant to ENSO are modeled. The NINO3 index is derived from these model runs as the average of the sea surface temperature

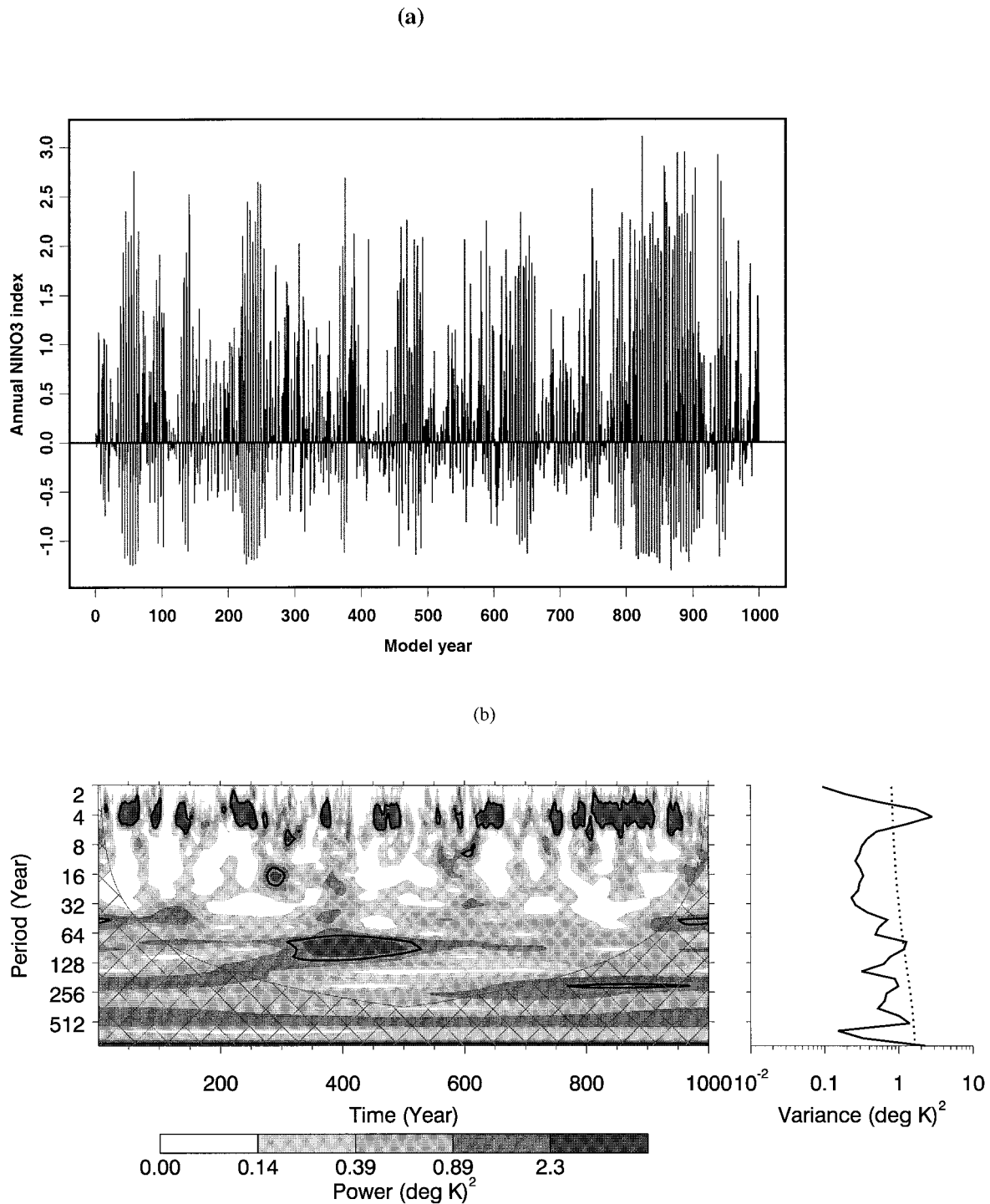


**Figure 4.** (a) Time series for a 1000-year segment of NINO3 variations from the *Zebiak and Cane* [1987] (ZC) coupled ocean-atmosphere model for ENSO. (b) Wavelet power spectrum for model NINO3. The contour levels are chosen so that 75%, 50%, 25%, and 5% of the wavelet power is above each level, respectively. The cross-hatched region shows the cone of influence, where zero padding has reduced the variance. The solid contour is the 10% significance level (with global wavelet spectrum as the background). On the right is the global wavelet power spectrum (solid line). The dotted line is the 10% significance level for the global wavelet spectrum (red-noise background). Wavelet analysis is based on *Torrence and Compo* [1998].

over the same region as for the historical data. In terms of the statistically significant frequencies the spectrum of the model-derived NINO3 is similar to that of the observation-based NINO3. The 110,000-year integration of the model was performed by Cane and Clement to develop a useful paleoclimate

perspective on ENSO. An interesting aspect of the results is the dramatic temporal variability in the computed NINO3 over decades, centuries, and millennia. A 1000-year segment of the model NINO3 index time series is shown in Figure 4a, and the corresponding wavelet spectra is shown in Figure 4b. It is

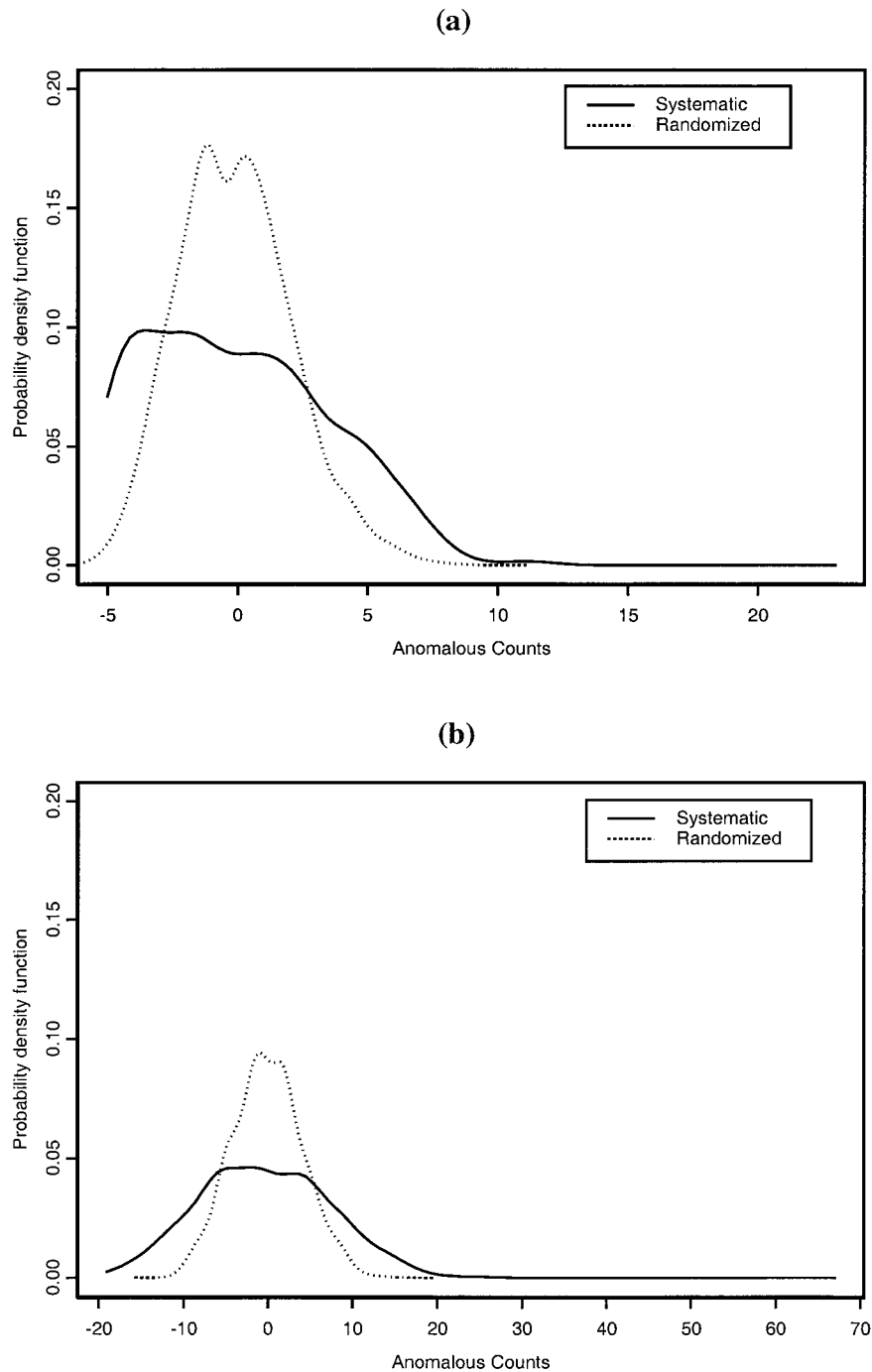


**Figure 5.** Probability distribution of anomalous La Niña occurrences from the 110,000 year run of the ZC model based on limited-length record: (a) 50 years and (b) 200 years. The probability distribution is computed using a Gaussian kernel, with normal optimal smoothing. The solid line represents a block bootstrap (systematic), and the dashed line represents a raw bootstrap (random). Note the fatter tail of the distribution where the time series structure is preserved (systematic).

interesting to note the manner in which the model spends long periods in a perpetual El Niño or La Niña state and also the changes in the frequency structure over time. The intermittency in the interannual band is reminiscent of the analysis of the 20th century, while the interdecadal and longer-period variations suggest possible modulating influences for the interannual variations. Such temporal variations are consistent with the behavior expected from moderately complex low-order

nonlinear dynamical systems and are discussed in the context of ENSO by *Tziperman et al.* [1994] and *Jin et al.* [1994]. It is not fully clear if the NINO3 realizations of this model over these timescales are representative of the real climate. However, it is interesting that even a relatively simple model for ENSO suggests highly nonstationary (both in the mean and the frequency structure) NINO3 variations. Thus the implication for ENSO-related hydrologic teleconnections (e.g., floods) is

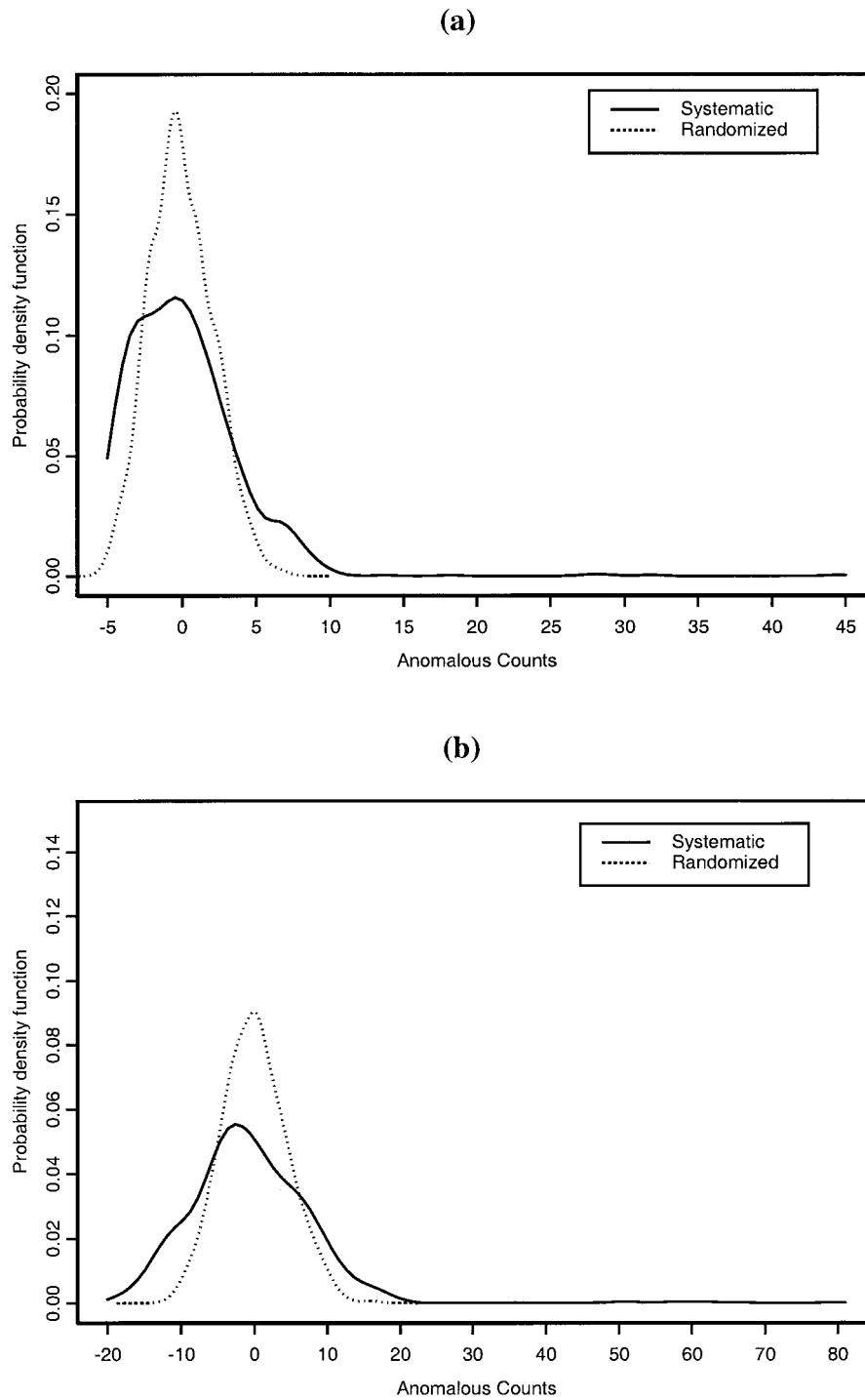


**Figure 6.** Same as Figure 5 but for El Niño conditions.

that even in the absence of climate forcing (e.g., stemming from increased  $\text{CO}_2$  influences) it is likely that there will be substantial variations (and potential nonstationarities) over timescales of interest for flood frequency analysis and water resources planning and management.

Given the complex time-frequency behavior and memory structure exhibited by the NINO3 in the model integrations, the ability to assess the behavior of hydroclimatic extremes given a sample of fixed sample size is not clear. Specifically, if the memory as inferred from traditional correlation and wave-

let analyses were limited to  $k$  years, a record of length  $n$  (sufficiently larger than  $k$ ) may, on average, still contain sufficient information about the long-term variations in extremes. In that case, for certain design and long-term flood planning activities, understanding and characterizing the memory in the flood-generating process may not be an overarching issue. For instance, analysis based on a 1000-year paleoflood record (where all the ENSO-driven structure in the flood process had a periodicity  $< 10$  years) would likely lead to flood quantile estimates consistent with the traditional flood frequency anal-

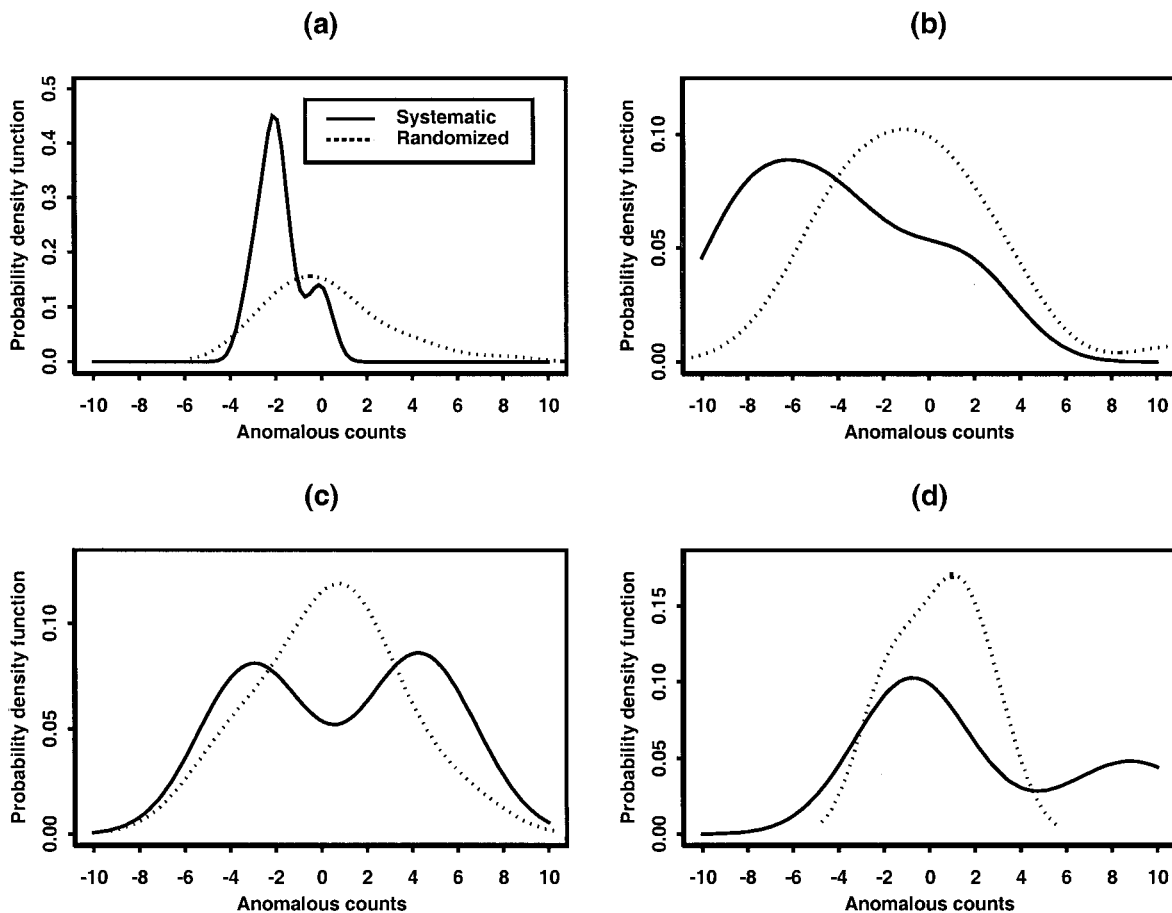


**Figure 7.** Probability distribution of the number of anomalous exceedances of the flood series based on a quantile threshold: (a)  $<10\%$ , (b)  $<33\%$ , (c)  $>67\%$ , and (d)  $>90\%$ . Quantiles are computed based on a 30-year time window, and exceedances of each quantile are computed for the next 30 years on record.

ysis assumptions. On the other hand, if the underlying generating process led to regime structure at multiple timescales (as suggested by the ZC model), it is not clear that an adequate record length will be easily established.

This issue is explored by examining the probability distribution of the frequency of occurrence of El Niño and La Niña events (i.e., extremes of the NINO3 process) for different sample sizes, drawn from the 110,000-year model NINO3 record. Both phases of ENSO are of interest since, depending on the location, the correlation of floods with NINO3 may be positive or negative. First, we define fixed thresholds of NINO3 values to define La Niña (NINO3 less than 10th percentile ( $-0.71$  K anomaly)) and El Niño (NINO3 greater than 90th percentile ( $1.8$  K anomaly)) events. Subsequently, we draw 1000 samples each of size 25, 50, 100, and 200 at random, with replacement (i.e., using a bootstrap procedure) from the 110,000-year record, and for each such sample we count the number of El Niño and La Niña events. We expect that a sample of size 200 may be adequate for robustly estimating the 10-year event (the 10th or 90th percentile of NINO3 in either direction) for an independent and identically distributed (i.i.d.) process.

Two sampling strategies are used. A “systematic” sample of length  $n$  is drawn as a contiguous block of  $n$  years from the 110,000-year record. This preserves the time series structure for a sample of that length and corresponds to a block boot-

strap. The second strategy entails drawing a sample of length  $n$  by randomly sampling  $n$  years from the 110,000-year record, corresponding to an ordinary bootstrap. The time series structure of the series is consequently not preserved. The probability distribution functions of the number of La Niña and El Niño events for a sample of size  $n$  for the systematic and random sampling designs are presented in Figures 5 and 6, respectively. The  $x$  axis in both Figures 5 and 6 records anomalous counts as the difference between the number of events in the sample and the average number of events across all samples of that size. We note that even for a record length of 200 years the distributions of the number of El Niño or La Niña events in systematic samples have a much fatter tail than the corresponding distribution for randomly sampled data. This observation suggests that if a flood process were closely tied to El Niño/La Niña occurrence, and the ZC model is representative of how these operate, the variability in the number of extreme (big or small) floods recorded in samples of typical length will be much greater than that expected under the i.i.d. assumption. Thus we can expect to be surprised more often than we expect, even with an apparently well-formulated and calibrated probability model for annual maximum floods, treated as stationary and independent from year to year.

Given this daunting perspective on long-term variability, we now explore whether a  $n$ -year flood period can be taken to be representative of the next  $n$  years. Two experiments are con-

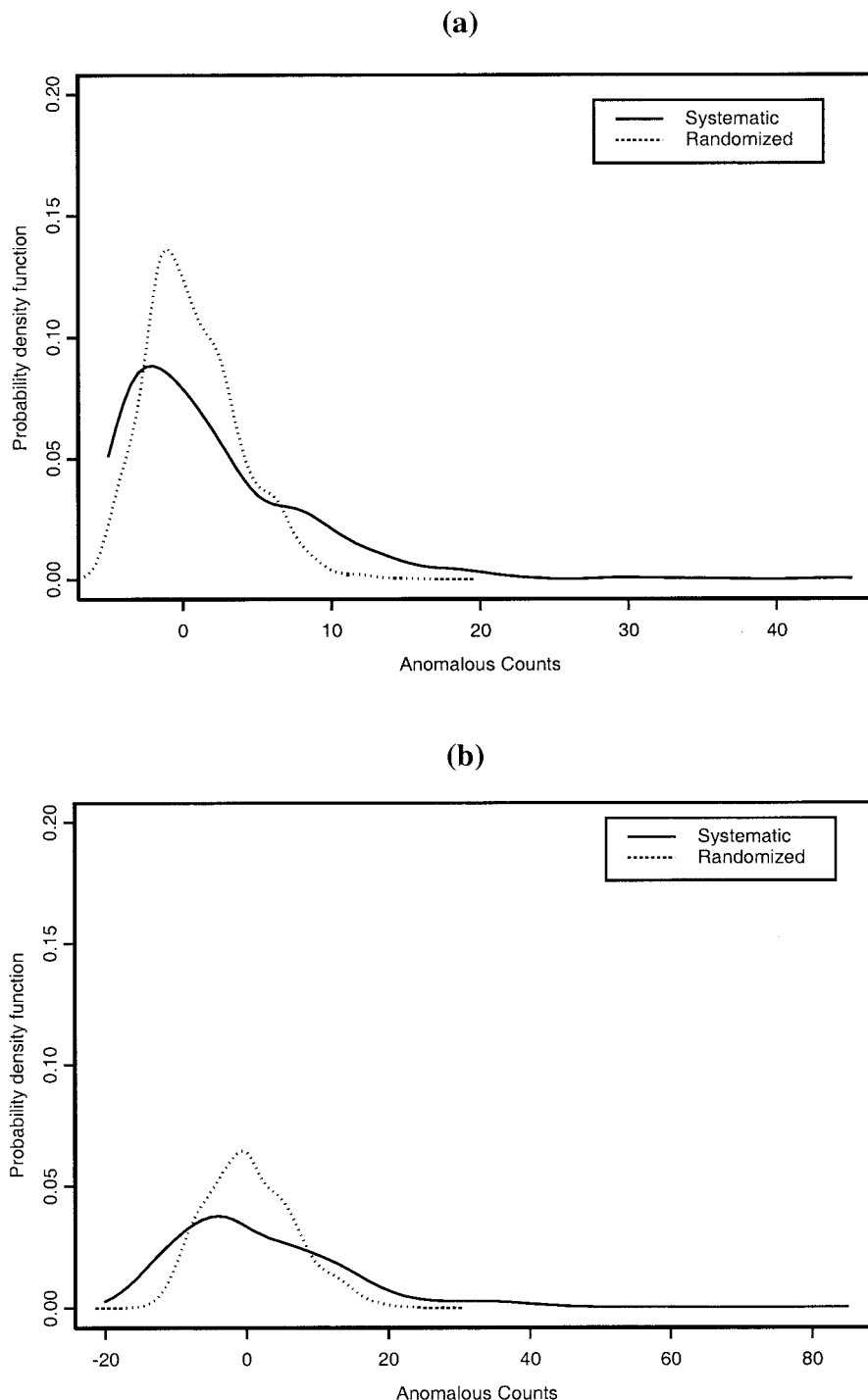


**Figure 8.** Probability distribution of the number of anomalous exceedances of the nintieth percentile of the ZC model NINO3 series for two successive  $n$  year periods using block or random sampling, where  $n$  is (a) 50 years and (b) 200 years. The probability distribution is estimated using a Gaussian kernel, with normal optimal smoothing. The solid line is for the block bootstrap, and the dotted line is for the raw bootstrap.

ducted: the first based on the flood data and the second with the ZC model NINO3 data.

The variation of the Similkameen River annual maximum flood series in successive 30-year periods is analyzed first. A 60-year segment of the record is selected randomly from the 88-year record. The annual maximum flows corresponding to the 10th, 33rd, 67th, and 90th percentiles of the first 30 years of this 60-year segment are estimated. We count the nonex-

ceedances of the 10th and 33rd percentiles and the exceedance of the 67th and the 90th percentile in the subsequent 30 years. This process is repeated for 29 available 60-year-long segments, and the resulting probability distribution of exceedances for each threshold is presented in Figure 7. The resulting frequency distribution is contrasted with the one obtained if each 30-year segment is drawn from the original record by randomly sampling each year rather than drawing a

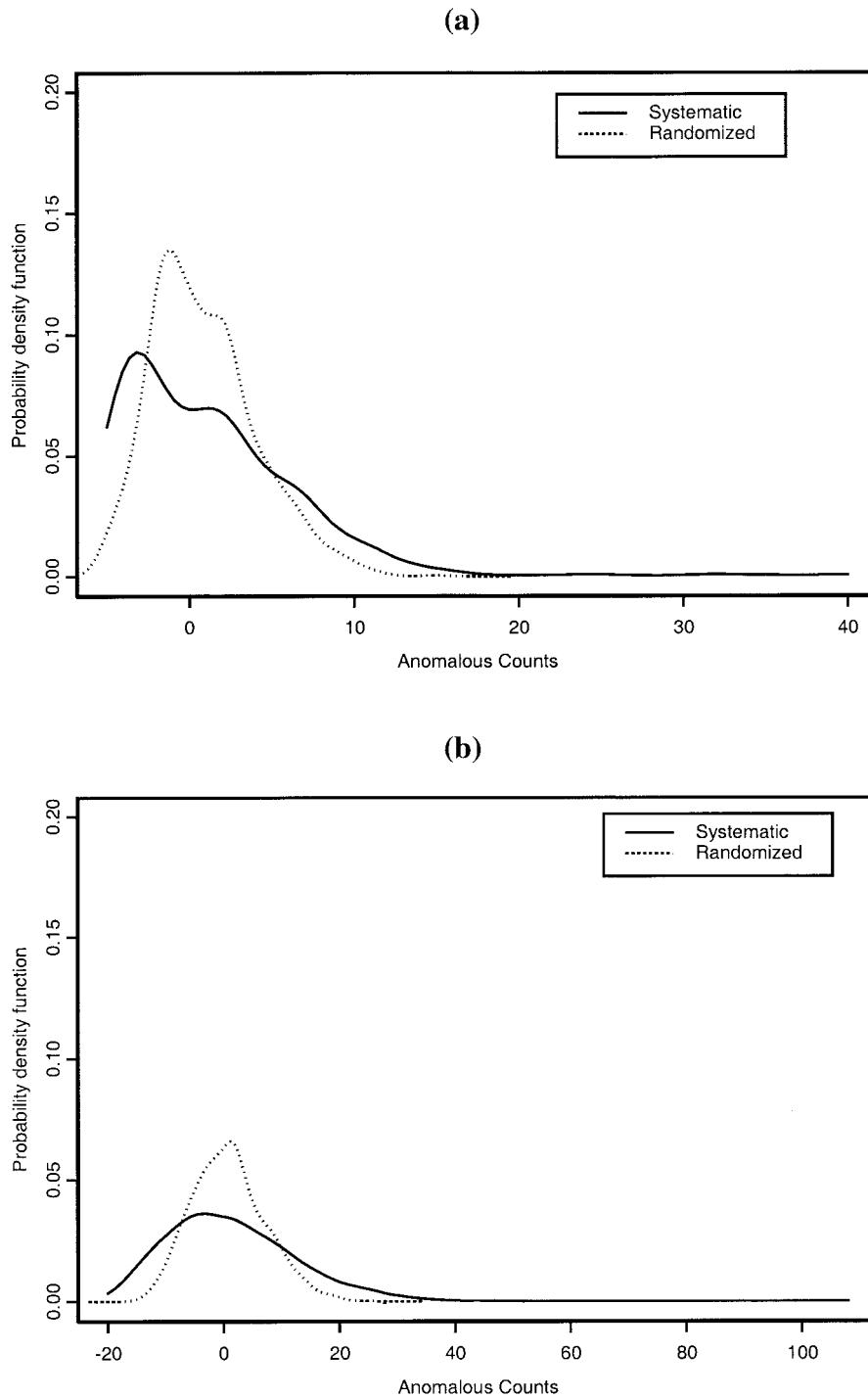


**Figure 9.** Same as Figure 8 but for nonexceedance of the 10th percentile of the ZC model NINO3.

contiguous 60-year block. There are rather large differences in the distributions of the systematic and randomized samples for the 10th, 33rd, and 90th percentiles. This is consistent with our intuition from the earlier analysis of the El Niño/La Niña event occurrence process using the model data and reinforces the notion that the role of nonstationarity in the time series is to lead to fatter-tailed distributions for the frequency of exceedance (i.e., the uncertainty distribution associated with the estimated flood frequency curve). Given the marked differences noted here, one would be hard pressed to accept the last 30 years as representative of the next 30 at this site.

We recognize that the 88-year record used above poses some severe constraints on the reliability of the resampling experiment that was conducted to assess the properties of exceedance. Consequently, the same experiment is now repeated for the NINO3 data (consider the hypothetical case that log (annual maximum flood) is perfectly correlated with NINO3) from the 110,000-year run of the ZC model. We consider the exceedance of the 90th percentile and the nonexceedance of the 10th percentile as estimated from the first  $n$  years and the second  $n$  years for samples of different size as before. The results (Figures 8 and 9) reinforce the earlier observations that

the time series structure imparts fatter tails to the exceedance/nonexceedance process.

## 6. Discussion

In this paper, we considered the time evolution of the annual maximum flood distribution and the possible modulating influence of the large-scale climate. The nearly century-long historical record for the Similkameen River shows marked interannual-to-interdecadal variations, resulting in some systematic variations in the flood potential. Such variations are not unique to this flood record as we noted in section 1. In closing, we offer the following observations and discuss some emerging research directions.

1. Flood potential is influenced by climate state, and the association between annual maximum floods and leading indicators of climate state can be identified.

2. Given the complex, low-frequency variations in climate state, flood frequency exhibits interannual, interdecadal, and longer variations that may be predictable, contingent on the predictability of the underlying climate state. Evidence was provided of the linear predictability of the annual maximum flood at the site studied nearly 4 months in advance. This information could be used for reservoir management for flood control and for near-term flood planning. The issue of longer-term prediction of climate and floods was not considered here.

3. The traditional assumption of stationarity in flood frequency analysis may translate into suboptimal decisions on flood control design given the large element of surprise indicated by the bootstrap analyses presented here. There is a much higher chance of seeing substantially different numbers of exceedances (nonexceedances) of the design flood based on the i.i.d. assumption once consideration is given to the long-term memory in the underlying process. The manner in which we develop an understanding of the incremental uncertainty and risk due to nonstationarity and use it in planning and design are questions worthy of further investigation. New perspectives on the relative merits of structural and nonstructural measures for flood control and for land use in the floodplain may emerge.

4. Models of climate, simple or complex but representative of the long-term variations of the system, will almost certainly be necessary to provide guidance for an assessment of the distribution of hydroclimatic extremes. The analysis presented here already provides some insights into new directions for analysis of flood frequency and factors of safety in design.

5. Hydrologic teleconnections to climate indicators and the associated atmospheric fluxes of water vapor exhibit considerable spatial and temporal structure. This is already understood through circulation pattern composites, linear statistical analysis (e.g., correlation), and numerical model analyses focused on events or periods of record. How do we move from this knowledge to a reassessment of regional/continental flood frequency that provides a proper context for reducing spatial and temporal flood risk? Since there is evidence that large regions may respond in a similar manner to climate precursors and may be mutually anticorrelated, opportunities for near-term resource allocation and insurance strategies that use such spatial information to adjust premiums and hence hedge risk are indicated. A new direction for the estimation of regional flood frequency, conditional on exogenous climate indices is also suggested.

6. For a practitioner an assessment of climate-related flood risk can provide useful insights into the revision of traditional

flood frequency estimation procedures and a better estimation and assessment of associated risk for water resources systems, dam safety, and floodplain management. In the absence of long hydrologic records a better understanding of the range of variability of climate precursors, their teleconnections, and an analysis of proxy records would help develop estimates of the possible flood risk, as well as some intuition as to how to interpret risk. At the same time, statistical-dynamical approaches that recognize the nature of teleconnections and sensitivity of flood response to climate may find useful applications in the area of climate-related flood risk assessment.

**Acknowledgments.** The work presented here was partially supported by the National Science Foundation through grants EAR 9973125 and EAR 9720134. S. Jain acknowledges support through the CIRES Visiting Fellows Program at NOAA-CIRES Climate Diagnostics Center. The authors wish to thank Mark Cane and Amy Clement for providing the model NINO3 data. The authors also thank the two anonymous reviewers for their helpful comments and suggestions regarding the presentation of results.

## References

- Barlow, M., S. Nigam, and E. H. Berbery, ENSO, Pacific decadal variability, and U.S. summertime precipitation, drought, and stream flow, *J. Clim.*, *14*, 2105–2128, 2001.
- Booy, C., and D. Morgan, The effect of clustering of flood peaks on a risk analysis for the Red River, *Can. J. Civ. Eng.*, *12*, 150–165, 1985.
- Cane, M. A., Tropical Pacific ENSO models: ENSO as a mode of the coupled system, in *Climate System Modeling*, edited by K. E. Trenberth, pp. 583–616, Cambridge Univ. Press, New York, 1992.
- Cane, M. A., and A. C. Clement, A role of the tropical Pacific coupled ocean-atmosphere system on Milankovitch and millennial time-scales, Part II, Global impacts, in *Mechanisms of Global Climate Change at Millennial Time Scales*, *Geophys. Monogr. Ser.*, vol. 112, edited by P. U. Clark, R. S. Webb, and L. D. Keigwin, pp. 373–383, AGU, Washington, D. C., 1999.
- Cayan, D. R., Interannual climate variability and snowpack in the western United States, *J. Clim.*, *9*, 928–948, 1996.
- Cayan, D. R., K. T. Redmond, and L. G. Riddle, ENSO and hydrologic extremes in the western United States, *J. Clim.*, *12*, 2881–2893, 1999.
- Clement, A. C., and M. A. Cane, A role of the tropical Pacific coupled ocean-atmosphere system on Milankovitch and millennial time-scales, Part I, A modeling study of tropical Pacific variability, in *Mechanisms of Global Climate Change at Millennial Time Scales*, *Geophys. Monogr. Ser.*, vol. 112, edited by P. U. Clark, R. S. Webb, and L. D. Keigwin, pp. 363–371, AGU, Washington, D. C., 1999.
- Cole, J. E., and E. R. Cook, The changing relationship between ENSO variability and moisture balance in the continental United States, *Geophys. Res. Lett.*, *25*, 4529–4532, 1998.
- Conover, W. J., *Practical Nonparametric Statistics*, 584 pp., John Wiley, New York, 1999.
- D'Arrigo, R., G. Wiles, G. Jacoby, and R. Villalba, North Pacific sea surface temperatures: Past variations from tree rings, *Geophys. Res. Lett.*, *26*, 2757–2760, 1999.
- Dettinger, M. D., D. R. Cayan, G. J. McCabe, and J. A. Marengo, Multiscale hydrologic variability associated with El Niño/Southern Oscillation, in *El Niño-Southern Oscillation: Multiscale Variability and Its Impacts on Natural Ecosystems and Society*, edited by H. F. Diaz, and V. Markgraf, pp. 113–148, Cambridge Univ. Press, New York, 2000.
- Dracup, J. A., and E. Kahya, The relationships between U.S. streamflow and La Niña events, *Water Resour. Res.*, *30*(7), 2133–2141, 1994.
- Gereshunov, A., and T. Barnett, ENSO influence on intraseasonal extreme rainfall and temperature frequencies in the contiguous United States: Observations and model results, *J. Clim.*, *11*, 1575–1586, 1998.
- Ghil, M., and R. Vautard, Interdecadal oscillations and the warming trend in global temperature time series, *Nature*, *350*, 324–327, 1991.
- Gu, D., and S. G. H. Philander, Interdecadal climate fluctuations that depend on exchanges between the tropics and extratropics, *Science*, *275*, 805–807, 1997.

- Guttman, N. B., Statistical descriptors of climate, *Bull. Am. Meteorol. Soc.*, 70, 602–607, 1989.
- Hastie, T., and C. Loader, Local regression: Automatic kernel carpentry, *Stat. Sci.*, 8(2), 120–143, 1993.
- Horel, J. D., and J. M. Wallace, Planetary scale atmospheric phenomena associated with the Southern Oscillation, *Mon. Weather Rev.*, 109, 813–829, 1981.
- Jain, S., and U. Lall, The magnitude and timing of annual maximum floods: Trends and large-scale climatic associations for the Blacksmith Fork River, Utah, *Water Resour. Res.*, 36(12), 3641–3652, 2000.
- Jain, S., U. Lall, and M. E. Mann, Seasonality and interannual variations of Northern Hemisphere temperature: Equator-to-pole gradient and ocean-land contrast, *J. Clim.*, 12, 1086–1100, 1999.
- Jin, F.-F., J. D. Neelin, and M. Ghil, El Niño on the devil's staircase: Annual subharmonic steps to chaos, *Science*, 264, 70–72, 1994.
- Kaiser, G., *A Friendly Guide to Wavelets*, 300 pp., Birkhäuser, Boston, Cambridge, Mass., 1994.
- Loader, C., *Local Regression and Likelihood*, 304 pp., Springer-Verlag, New York, 1999.
- Mann, M. E., R. S. Bradley, and M. K. Hughes, Long-term variability in the El Niño Southern Oscillation and associated teleconnections, in *El Niño-Southern Oscillation: Multiscale Variability and Its Impacts on Natural Ecosystems and Society*, edited by H. F. Diaz, and V. Markgraf, pp. 357–412, Cambridge Univ. Press, New York, 2000.
- Mantua, N. J., S. T. Hare, Y. Zhang, J. M. Wallace, and R. C. Francis, A Pacific interdecadal climate oscillation with impacts on Salmon production, *Bull. Am. Meteorol. Soc.*, 78, 1069–1079, 1997.
- McCabe, G. J., and M. D. Dettinger, Decadal variations in the strength of the ENSO teleconnections with precipitation in the western United States, *Int. J. Climatol.*, 19, 1399–1410, 1999.
- Minobe, S., A 50–70 year climatic oscillation over the North Pacific and North America, *Geophys. Res. Lett.*, 24, 683–686, 1997.
- National Research Council, *Decade-to-Century-Scale Climate Variability and Change: A Science Strategy*, Panel on Clim. Variability on Decade-to-Century Time Scales, 160 pp., Natl. Acad. Press, Washington, D. C., 1998.
- National Research Council, *Improving American River Flood Frequency Analyses*, 120 pp., Natl. Acad. Press, Washington, D. C., 1999.
- Olsen, J. R., J. R. Stedinger, N. C. Matalas, and E. Z. Stakhiv, Climate variability and flood frequency estimation for the upper Mississippi and lower Missouri rivers, *J. Am. Water Resour. Assoc.*, 35(6), 1509–1523, 1999.
- Rajagopalan, B., U. Lall, and M. Cane, Anomalous ENSO occurrences: An alternate view, *J. Clim.*, 10, 2351–2357, 1997.
- Rajagopalan, B., E. Cook, U. Lall, and B. K. Ray, Spatiotemporal variability of ENSO and SST teleconnections to summer drought over the United States during the twentieth century, *J. Clim.*, 13, 4244–4255, 2000.
- Robson, A. J., T. K. Jones, D. W. Reed, and A. C. Bayliss, A study of national trend and variation in UK floods, *Int. J. Climatol.*, 18, 165–182, 1998.
- Ropelewski, C. F., and M. S. Halpert, Global and regional scale precipitation patterns associated with the El Niño/Southern Oscillation, *Mon. Weather Rev.*, 115, 1606–1626, 1987.
- Slack, J. R., J. M. Landwehr, and A. Lumb, A U.S. Geological Survey streamflow data set for the United States for the study of climate variations, 1874–1988, *U.S. Geol. Surv. Open File Rep.*, 92-129, 1992.
- Torrence, C., and G. P. Compo, A practical guide to wavelet analysis, *Bull. Am. Meteorol. Soc.*, 79, 61–78, 1998.
- Trenberth, K. E., and C. J. Guillemot, Physical processes involved in the 1988 drought and 1993 floods in North America, *J. Clim.*, 9, 1288–1298, 1996.
- Trenberth, K. E., and T. Hoar, The 1990–1995 El Niño-Southern Oscillation event: Longest on record, *Geophys. Res. Lett.*, 23, 57–60, 1996.
- Trenberth, K. E., G. W. Branstator, D. Karoly, A. Kumar, N.-C. Lau, and C. Ropelewski, Progress during TOGA in understanding and modeling global teleconnections associated with tropical sea surface temperatures, *J. Geophys. Res.*, 103(7), 14,291–14,324, 1998.
- Tziperman, E., L. Stone, M. Cane, and H. Jarosh, El Niño chaos: Overlapping of resonances between the seasonal cycle and the Pacific ocean-atmosphere oscillator, *Science*, 264, 72–74, 1994.
- Urban, F. E., J. E. Cole, and J. T. Overpeck, Influence of mean climate change on climate variability from a 155-year tropical Pacific coral record, *Nature*, 407, 989–993, 2000.
- Walker, F. R., and J. R. Stedinger, Long-term variability in the arrival rate of flood events as evidenced by flood clustering, *Eos Trans. AGU*, Spring Meet. Suppl., 81(19), H 31D-02, 2000.
- Zebiak, S. E., and M. A. Cane, A model for the El Niño-Southern Oscillation, *Mon. Weather Rev.*, 115, 2262–2278, 1987.
- Zhang, Y., J. M. Wallace, and N. Iwasaka, Is climate variability over the North Pacific a linear response to ENSO?, *J. Clim.*, 9, 1468–1478, 1996.
- Zhang, Y., J. M. Wallace, and D. Battisti, ENSO-like interdecadal variability: 1900–1993, *J. Clim.*, 10, 1004–1020, 1997.

S. Jain, NOAA-CIRES Climate Diagnostics Center, R/CDC1, 325 Broadway, Boulder, CO 80305, USA. (sjain@cdc.noaa.gov)

U. Lall, Department of Earth and Environmental Engineering, Columbia University, New York, NY 10027, USA. (ula2@columbia.edu)

(Received March 5, 2001; revised September 18, 2001; accepted September 20, 2001.)

